

Steven M. Hunter, Edmond W. Holroyd, III, and Curtis L. Hartzell  
U.S. Bureau of Reclamation, Denver, CO

## 1. INTRODUCTION

During the period 1991-1997, approximately 160 WSR-88D (Weather Surveillance Radar - 1988 Doppler) radars were installed in the United States (U.S.) and abroad (Crum et al. 1993). The WSR-88D's operational precipitation algorithms, collectively known as the Precipitation Processing Subsystem (PPS), were designed for rain rather than snow (Fulton et al. 1998).

In 1995 the Bureau of Reclamation (Reclamation) was tasked by the WSR-88D Operational Support Facility (OSF) to develop a snow accumulation algorithm (SAA), and did so in the succeeding three years. This SAA was designed for use with dry (not melting) snow. The results were published in Super and Holroyd (1998).

Under the auspices of the GEWEX Continental-Scale International Program (GCIP; Coughlan and Avissar 1996) and Reclamation's Science and Technology Program, a version of the SAA was developed to utilize real-time Level III data. This version was deployed in the north-central United States (U.S.) as a demonstration project during cool seasons from 1998-2001, providing graphical distributions of snow water equivalent (SWE) and snow depth (SD) estimates on the Internet.

Recently the SAA was improved by several major modifications. These changes, which primarily identify different precipitation types, are the subject of this paper.

## 2. VERTICAL REFLECTIVITY PROFILE CORRECTION

In the SAA, the relationship between equivalent radar reflectivity  $Z_e$  and snowfall rate  $S$  is approximated by the same power law used for rainfall, except that snowfall rate  $S$  is substituted for rainfall rate  $R$ , i.e.,  $Z_e = \alpha S^\beta$ . For dry snow,  $\beta = 2.0$  was found to be appropriate for several locations and a change in  $\beta$  of  $\pm 0.2$  had little practical significance (Super and Holroyd 1998). In the north-central U.S.,  $\alpha$  was set to 150. Further, a seasonal-average range correction scheme was applied at ranges ( $r$ ) beyond 35 km, because the accuracy of snow estimates degrades as  $r$  increases. The correction factor (CF) was  $1.04607 - (0.0029590 \times r) + (0.0000506 \times r^2)$ . This methodology had problems, however, including bright band contamination and virga. The SAA also allowed changes to minimum and maximum  $\text{dbZ}_e$  values for precipitation calculations, and to WSR-88D hybrid scan and occultation files.

The SAA calibrates to  $Z_e$  rather than  $Z$  as in the rainfall equation because of non-Rayleigh scattering of incident radar energy by snow. The change of  $Z_e$  with

height is called the vertical profile of reflectivity or VPR. The importance of some type of VPR correction is reinforced by the literature. Joss & Waldvogel (1990) assert that VPR measurement is "...the main problem in using radar for precipitation measurements and hydrology in operational applications." This is affirmed by several researchers, including Koistinen (1991), Galli and Joss (1991), Andrieu and Creutin (1991), Smith (1990), and Joss and Waldvogel (1990). Hunter (1996) reiterated this finding for the operational WSR-88D.

The problem is that, under normal refractivity, radar beams become increasingly elevated with greater radar range, so the full VPR is not sampled. This situation is exacerbated by many stratiform rain and snowfall events, which are shallow and tend to have maximum  $Z_e$  values near the terrain (Joss and Lee 1995). The sampling beam may even be partially filled by hydrometeors, further reducing  $Z_e$  and  $S$ . See Fig. S1 for illustration.

The initial range correction was formulated by constructing a VPR, then converting the vertical position to an equivalent range using standard beam refraction (Holroyd 1999). This VPR is a mean profile from 35 km range in nine snowstorms near Minneapolis, and has a linear decrease of about 20% in  $Z_e$  per km altitude. Such an approach is supported by Joss and Waldvogel (1989), and Vignal et al. (2000), who assert that even a crude seasonal estimate can significantly improve precipitation estimates at mid-to-far ranges.

The VPR and range correction can be considered equivalent, except when precipitation estimates are derived with  $Z_e$  data from other than the lowest  $0.5^\circ$  radar tilt. This situation occurs when there is sufficient terrain blockage of this tilt to cause data collection from the  $1.5^\circ$  or higher tilts. Tilt selection is determined by the radar's hybrid scan strategy, as described by O'Bannon (1997). In areas with blockage near the radar, such as in Montana, upper tilt usage increased partial beam filling and consequent underestimation. This underestimation was not adequately compensated by the range CF; therefore, a true VPR correction was needed. This correction,  $F_c$ , uses an  $\alpha_c$  based upon the clearance,  $C$ , between beam center and the ground.

The snow precipitation rate, using  $\alpha$  and  $\beta$  appropriate to the precipitation type, is

$$S = F_c * (Z_e/\alpha)^{1/\beta} \quad (1)$$

where  $F_c = (\alpha/\alpha_c)^{1/\beta} = (150/\alpha_c)^{1/2.0}$  (2) and where 150 and 2.0 are from the original SAA for the north-central U.S. This results in

$$\alpha_c = \exp(-0.0004092687 * C + 5.225943), \text{ or} \\ \ln(\alpha_c) = -0.0004092687 * C + 5.225943. \quad (3)$$

In the VPR correction,  $\alpha_c$  decreases with  $C$ . Thus a smaller  $\alpha$  will be applied not only if data are taken from

\* Corresponding author address: Steven M. Hunter, Bureau of Reclamation, D-8510, Denver Federal Center, PO Box 25007, Denver, CO, 80225-0007; e-mail: smhunter@do.usbr.gov

increasing range with the first tilt ( $0.5^\circ$ ), but also if taken from the second ( $1.5^\circ$ ) or higher tilts. Either application will compensate for lack of beam filling. The  $\alpha$  vs  $C$  profile is a linear least squares fit to 21 data points from four sites - Minneapolis, Albany, Denver and Cleveland, as portrayed in Fig. 1. See Fig. S2 for an illustration of the differences between new and old corrections.

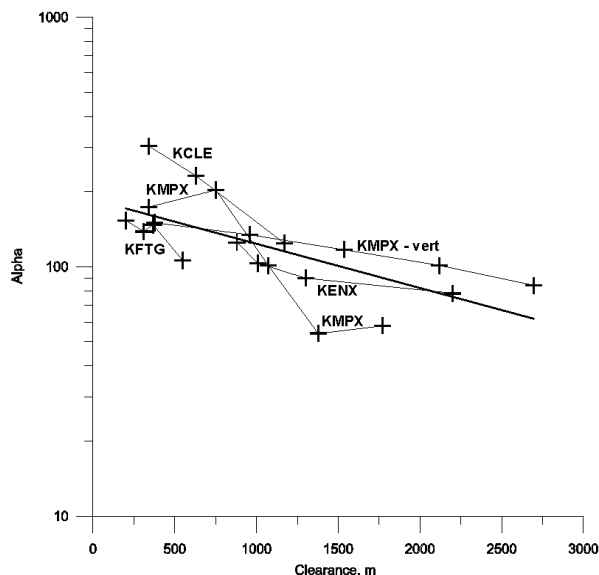


**Figure 1.** Relation between  $\alpha$  and beam clearance for several radars. Thick line is a linear least squares fit. VPR used for the previous range correction is included for reference (KMPX-vert).

### 3. PRECIPITATION TYPE CLASSIFICATION

Mixed-phase precipitation has been a major hindrance to SAA accuracy. Since the algorithm was designed for dry snow only and when the freezing level is above the WSR-88D's antenna height, radar bright band contamination generally results in significant radar precipitation overestimation. Consequently, a simple method was developed to identify such cases and segregate different precipitation regimes.

#### 3.1 Liquid, Solid, and Bright Band Classification

Cases with obvious bright band contamination were analyzed to develop a precipitation-typing scheme. The altitude of the top of the bright band, where there was an abrupt downward increase in reflectivity, was determined at near-to-intermediate (40-150 km) ranges using all four lower tilts.

At altitudes just below the  $0^\circ\text{C}$  level, melting ice (the bright band) exists and nearly any thermal profile is possible, including more than a 1 km thickness of near-isothermal air, and multiple inversions. In the studied bright band cases the altitude of the bottom of the bright band, where there was an abrupt upward increase in reflectivity, was noted and compared with temperatures from rawinsondes. The temperature of the bottom of the bright band was usually about  $+4^\circ\text{C}$ . This is in agreement with typical experiences at the surface, where

wet snow is seldom seen at air temperatures warmer than  $+4^\circ\text{C}$ . Though this threshold is more variable than the melting level, a transition from melting ice to rain is declared to be at the *lowest* altitude of  $+4^\circ\text{C}$ , i.e., pure rain is assumed if the top of the radar beam is entirely below this altitude. In this instance, a Z-R instead of Z-S relationship should be used to produce rainfall rates. As suggested by results near Albany, NY, however, these two relationships may not be substantially different (Super and Holroyd 1998).

In the new algorithm, any beam sampling the layer between  $0^\circ\text{C}$  and  $+4^\circ\text{C}$  is assumed to be contaminated by bright band effects. These data require a markedly different relationship between reflectivity and precipitation rate. The inclusion of different precipitation types (snow, melting snow, rain), led to renaming the SAA as the Precipitation Accumulation Algorithm (PAA). At present the PAA flags melting-level radar data bins as contaminated and uses an arbitrary set of adaptable parameters to estimate precipitation. A few case studies suggest  $\alpha = 300$  and  $\beta = 2.0$ . Coding might be added to estimate the proportion of the beam contaminated by the bright band, thereby decreasing the bright band correction with range. We adopted this approach because of the large temporal and spatial variability of bright band structure observed in the north-central U.S. Fabry and Zawadzki (1995) also reported great variability in bright band intensities.

Once the precipitation type (snow, melting snow, or rain) is determined, the most appropriate Z-R (or Z-S) equation is applied to calculate a precipitation amount for a radar bin. This amount is then extrapolated to the surface, using the climatological VPR and bin clearance  $C$ . Then, from the terrain file, the surface elevation under the bin is determined and its temperature obtained from a forecast model sounding. This temperature is compared to the  $0^\circ\text{C}$  and  $+4^\circ\text{C}$  thresholds and, using the same logic as the radar bin sample, a "final" precipitation type at the surface is prescribed. Fig. S3 shows an example of this scheme. No snow depth (SD) is accumulated in areas of rain. For areas of melting snow a larger snow density  $\rho$  is used for SD, compared to  $\rho$  in areas of dry snow.

The  $0^\circ\text{C}$  and  $4^\circ\text{C}$  altitudes are obtained from numerical weather prediction (NWP). NWP models have recently offered vertical profiles of temperature and dew point ("model soundings") at hourly forecast intervals, much more frequent than 12-hourly rawinsondes. Moreover, model soundings are available for many more locations than rawinsonde soundings, including several WSR-88D locations not collocated with upper-air sites. A single model sounding per forecast hour is used for all data under a particular radar's coverage umbrella.

Forecast sounding files are automatically obtained via FTP from the National Centers for Environmental Prediction's Eta model (22 km horizontal resolution) for the 0000, 0600, 1200, and 1800 UTC runs. Since these data become available 2-3 hours after the run cycles, soundings from 3 - 9 hour forecast times are nominally used (at 9 hours the next run becomes available). From each hourly sounding, the highest  $0^\circ\text{C}$  and lowest  $+4^\circ\text{C}$

levels are calculated for the precipitation type determination within the algorithm. If such levels are below ground at the sounding site, they are determined by extrapolating the temperature downward at the dry adiabatic lapse rate. The precipitation type procedure is subject to NWP errors that can adversely affect the altitude of relevant bright band elevations.

### 3.2 Virga Identification

Virga, or precipitation that is not reaching the ground, has been a continuing problem for the SAA and PPS. This problem is greatest at far ranges, where the lowest radar beam senses precipitation in the middle troposphere and/or when a dry sub-cloud atmosphere causes evaporation or sublimation. On a conventional PPI display, virga causes a “donut” pattern that indicates echoes almost exclusively at far range and high elevations (Holroyd 1999). The new algorithm applies two tests for possible virga.

First, from the model sounding a mean relative humidity (RH) is extracted for each 1.5 km layer above the terrain at every radar bin location. If that RH is less than a threshold, indicating dry air in low layers, a virga class flag is set and the VPR correction is not made at that bin, avoiding an increase in the surface precipitation estimate. The current threshold of 70% is considered conservative, to prevent elimination of valid surface precipitation. If the layer RH is less than this threshold, a second, radar-based technique is executed every volume scan to refine testing for the presence of virga.

For the radar-based technique, a cylindrical volume is defined (Fig. 2) by adaptable parameters (defaults indicated) for range (100 km), bottom (0.2 km) and top (1.5 km) with respect to the radar location and altitude. The 0.2 km bottom level was chosen to reduce the contribution of anomalous propagation echoes. The fraction of the hybrid scan’s radar bins within the cylinder that have a reflectivity greater than a specified minimum (0 dBZ<sub>e</sub>) is then computed. If that fraction is less than a threshold (currently 0.05) and the dry air class flag for a range bin is set, virga is probable and precipitation is zeroed for ranges beyond the cylinder. Echoes within the cylinder are treated normally unless the dry air flag is set, in which case the echo contribution to precipitation is permitted but not augmented by the VPR correction.

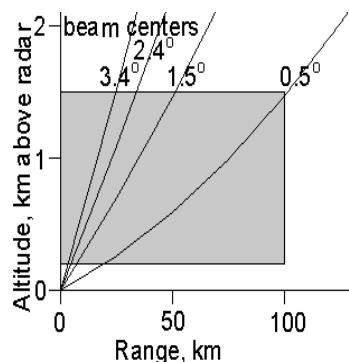


**Figure 2.** Schematic illustrating virga-testing cylindrical volume with 100 km range and 0.2-1.5 km altitude dimensions, and radar beam geometries.

### 3.3 Output Products

The PAA continues to output SWE and SD for optional periods of 1, 3, 6, and 24 hours. A new classification product identifies precipitation type within the radar beam, the type at the surface, and the possible presence of virga. An optional time-height diagram of temperature, RH, and maximum echo is available for the lowest 3 km above the radar. For the north-central U.S. during the cool season (October-April), real-time products are posted on the Internet at [yampa.earthsci.do.usbr.gov:8080/awards/Mn/index.html](http://yampa.earthsci.do.usbr.gov:8080/awards/Mn/index.html)

## 4. SUMMARY

- The former SAA range correction employed a mean VPR recast as a function of range. The PAA restores the adjustment with a true VPR, based on clearance between a radar beam center and the terrain.
- Precipitation phase in the radar beam and at the surface is classified into three types: dry snow, melting snow (slush), and rain, based on hourly model sounding altitudes of the highest 0°C and lowest +4°C levels. If any part of the radar beam is between those altitudes, it is considered contaminated by bright band effects. If the surface temperature is warmer than +4°C, snow depth SD is not accumulated because rain is assumed. The three classes can have different  $\alpha$ , but  $\beta$  remains 2.0.
- Two tests were developed to reduce virga contamination of the precipitation products. The first tests for low-level dry air using RH from model soundings. If such dry air exists, a second, radar-based test determines if low-level echoes of a specified intensity are sufficiently numerous to permit echoes to produce precipitation at far range.
- Output products are liquid equivalent precipitation SWE, additional SD, precipitation class, and time-height diagrams of various parameters.

## ACKNOWLEDGMENTS

Thanks to Ra Aman for programming support. This work was funded by the NEXRAD Operational Support Facility (now Radar Operations Center), Reclamation’s Science & Technology program, and NOAA’s GCIP.

## REFERENCES

- Andrieu, H., and J.D. Creutin, 1991: Effect of the vertical profile of reflectivity on the rain rate assessment at ground level. Preprints, *25th Intl. Conf. on Radar Meteor.*, Amer. Meteor. Soc., Boston, 832-835.
- Coughlan, M. and R. Avissar, 1996: The Global and Energy Water Cycle Experiment (GEWEX)

- Continental-Scale Intl. Project (GCIP): An Overview. *J. Geophys. Res.*, **101**, 7139-7148.
- Crum, Timothy D., R.L. Alberty, 1993: The WSR-88D and the WSR-88D Operational Support Facility. *Bull. Amer. Meteor. Soc.*, **74**, 1669-1688.
- Fabry, F., and I. Zawadzki, 1995: Long-term radar observations of the melting layer of precipitation and their interpretation. *J. Atmos. Sci.*, **52**, 838-851.
- Fulton, R.A., J.P. Breidenbach, D.J. Seo, D.A. Miller, and T. O'Bannon, 1998: The WSR-88D rainfall algorithm. *Wea. Forecasting*, **13**, 377-395.
- Galli, G., and J. Joss, 1991: Using and adjusting conventional radar reflectivity data for estimation of precipitation: past, present and future studies in Switzerland. In *Hydrological Applications of Weather Radar*, I.D. Cluckie and C.G. Collier Eds. Ellis Horwood, Chichester England, 65-73.
- Holroyd, E.W., 1999: *Snow accumulation algorithm for the WSR-88D radar: supplemental report*. Bureau of Reclamation Report R-99-11, Denver, Colorado, June, 30 pp.
- Hunter, S.M., 1996: WSR-88D radar rainfall estimation: Capabilities, limitations and potential improvements. *Natl. Wea. Dig.*, **20**, 26-38.
- Joss, J., and A. Waldvogel, 1989: Precipitation estimates and vertical reflectivity profile corrections. Preprints, *24th Conf. on Radar Meteor.*, Amer. Meteor. Soc., 682-688
- Joss, J., and A. Waldvogel, 1990: Precipitation measurements and hydrology. In *Radar in Meteor.*, D. Atlas Ed. Amer. Meteor. Soc., Boston, 577-606.
- Joss, J., and R. Lee, 1995: The application of radar-gage comparisons to operational precipitation profile corrections. *J. Appl. Meteor.*, **34**, 2612-2630.
- Koistinen, 1991: Operational correction of radar rainfall errors due to the vertical reflectivity profile. Preprints, *25th Intl. Conf. on Radar Meteor.*, Amer. Meteor. Soc., Boston, 91-94.
- O'Bannon, T., 1997: Using a 'terrain-based' hybrid scan to improve WSR-88D precipitation estimates. Preprints, *28th Conf. on Radar Meteor.*, Austin, TX, Amer. Meteor. Soc., 506-507.
- Smith, P.L., 1990: Precipitation measurement and hydrology: Panel report. In *Radar in Meteor.*, D. Atlas Ed. Amer. Meteor. Soc., Boston, 607-618.
- Super, A.B., and E.W. Holroyd, 1998: *Snow Accumulation Algorithm for the WSR-88D Radar: Final Report*. Bureau of Reclamation Report R-98-05, Denver, Colorado, June, 75 pp.
- Vignal, B., G. Galli, J. Joss, and U. Germann, 2000: Three methods to determine profiles of reflectivity from volumetric radar data to correct precipitation estimates. *J. Appl. Meteor.*, **39**, 1715-1726.
- 
- PAA verification and parameter refinement by case study continues and results will be included in a final report to GCIP in late May, 2001. Copies of this report may be obtained by contacting the corresponding author.

## Supplemental Figures

### Sectorized Hybrid Scan For radials with blockage

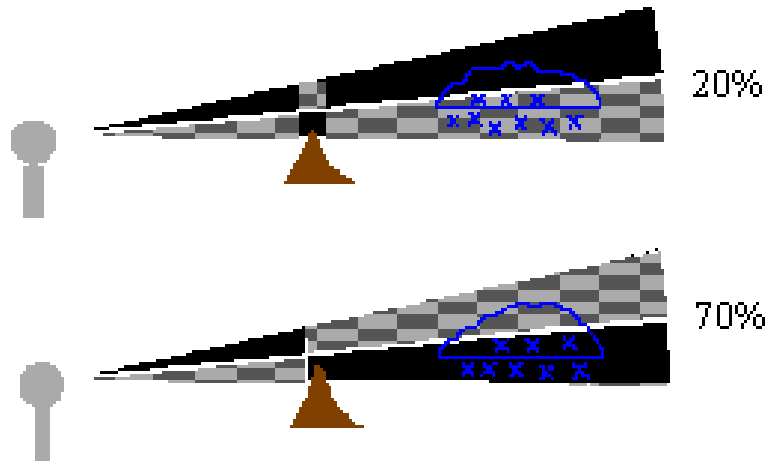


**Figure S1.** Examples of hybrid scan and its possible effect on S. Top shows small amount (20%) of blockage of lowest beam so that data is still gathered beyond the blockage (checkerboard beam). Bottom shows large amount (70%) of blockage of the lowest beam so that data are no longer collected from that beam (black beam) but rather the next beam above. Blue outline and "X's" connote shallow cloud and snow particles respectively.

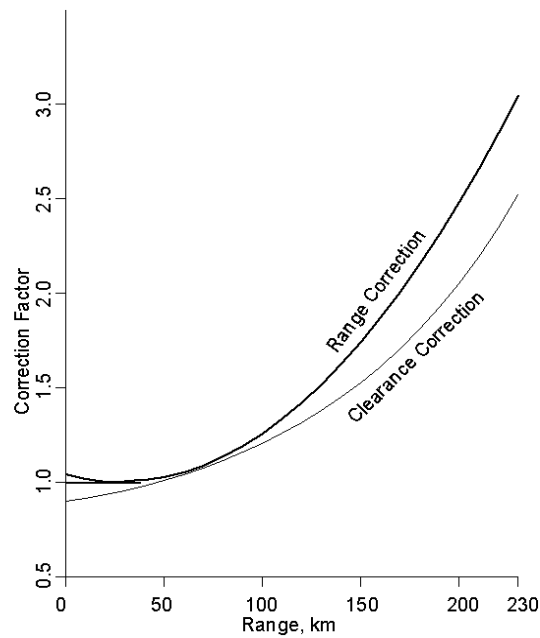


**Figure S2.** Range and clearance correction factors as a function of range for the 0.5 degree beam, for old range correction and new clearance correction, both with  $\alpha = 150$ , and  $\beta = 2.0$ .

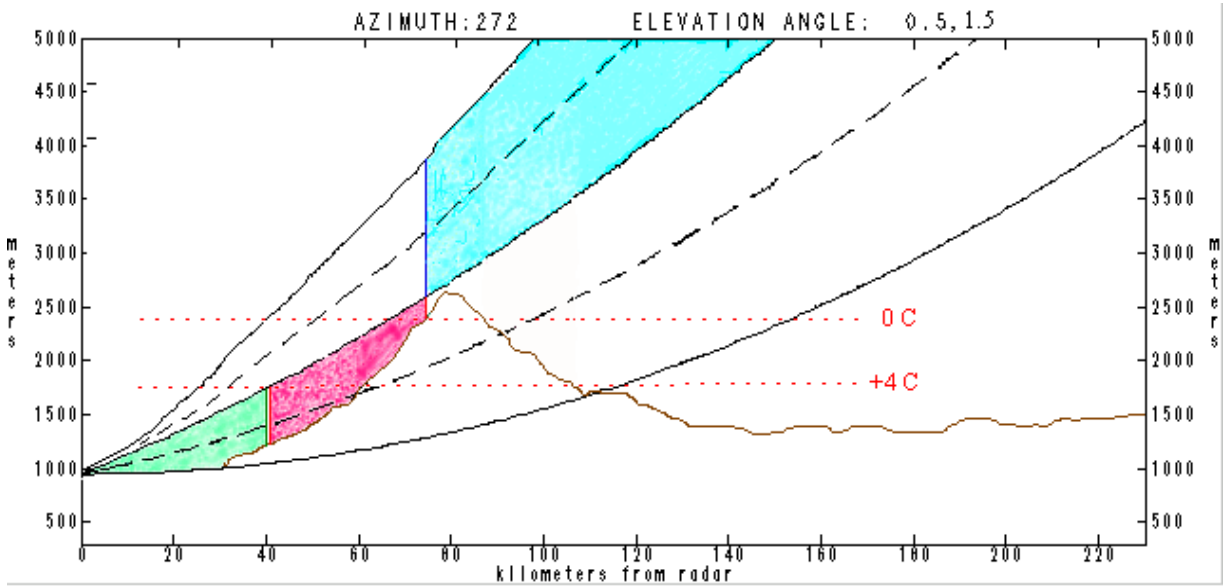


**Figure S3.** Hypothetical diagram of precipitation-typing logic of PAA. Altitudes of threshold temperatures are given by dotted red lines and terrain by brown line. Extent of 0.5° and 1.5° beams are solid black lines and their centers are dashed black lines. Green, red, and blue areas represent beam samples producing rain, bright band, and snow, respectively. Snow samples are taken from the 1.5° beam, as prescribed by the hybrid scan. Other samples are from the 0.5° beam.